DISCRETIZING TRANSIENT CURRENT DENSITIES IN THE MAXWELL EQUATIONS*

Mark L. Stowell, Daniel A. White,†
Lawrence Livermore National Laboratory, P.O. Box 808, Livermore CA, 94551, USA

Abstract

We will briefly discuss a technique for applying transient volumetric current sources in full-wave, time-domain electromagnetic simulations which avoids the need for divergence cleaning. The method involves both "edge-elements" and "face-elements" in conjunction with a particle-in-cell scheme to track the charge density. Results from a realistic, 6.7 million element, 3D simulation are shown. While the authors may have a finite element bias the technique should be applicable to finite difference methods as well.

INTRODUCTION

The Maxwell Equations

The Maxwell Equations with a current density source term can be written

$$\begin{aligned} \frac{\partial}{\partial t}\vec{D} &= \nabla \times \vec{H} - \vec{J} \\ \frac{\partial}{\partial t}\vec{B} &= -\nabla \times \vec{E} \end{aligned}$$

where

$$\vec{D} = \epsilon \vec{E} \text{ and } \vec{B} = \mu \vec{H}$$

These equations are commonly discretized using "edge-elements", or discrete 1-forms, for the electric field and "face-elements", or discrete 2-forms, for the magnetic flux density. This scheme requires that $\vec{J}$ also be approximated with edge-elements, which works quite well in many situations. However, this scheme does have certain drawbacks.

One difficulty with 1-form current densities is that they can spread through material interfaces into non-physical regions. For example, consider a vacuum region abutting a weak conductor which contains a constant current density. What value for $\vec{J}$ should be applied to the edges which are shared between these two regions? If the constant $\vec{J}$ value is used, then the conducting region will contain the correct value but the vacuum region will also contain a non-zero current density. If a value of zero is applied on these edges, then the vacuum region will correctly have zero current but the conductor will contain less current density than desired.

Another difficulty, and the one we will focus on, arises if the current density is transient and the primary interest is to determine how a cavity will resonate after a current pulse passes through it. The problem here is that the continuity equation for the electric charge,

$$\frac{\partial \rho}{\partial t} + \nabla \cdot \vec{J} = 0,$$

is only weakly satisfied. Therefore, current densities can, and often do, leave behind non-physical charge densities after they pass through the computational mesh. These charge densities can, in turn, produce a non-physical, static, electric field which not only adds unexpected, mesh dependent, features to field plots but can also reduce the accuracy of the meaningful portion of the solution.

Integrating the charge continuity equation over time we obtain

$$\rho(t_b) - \rho(t_a) = -\int_{t_a}^{t_b} \nabla \cdot \vec{J} dt.$$

Assuming t_a and t_b are chosen such that $\vec{J}$ is everywhere equal to zero before t_a and after t_b with no charges being left behind anywhere within the problem domain we would have $\rho(t_a) = \rho(t_b) = 0$ and so

$$\int_{t_a}^{t_b} \nabla \cdot \vec{J} dt = 0.$$

This is the constraint that we hope to satisfy. The accuracy with which this can be accomplished will hinge on our ability to accurately represent the divergence of the vector flux density $\vec{J}$.

Discrete Differential Forms

Differential Forms provide a general mathematical formalism to describe not only Div, Grad, and Curl but also integral relationships like the fundamental theorem of calculus, Kelvin-Stokes theorem, and the Divergence theorem. For example these three theorems can each be described by the generalized Stokes' theorem:

$$\int_{\Omega} d\omega = \oint_{\partial\Omega} \omega \qquad (1)$$

Where "ω" is a differential form and "d" is the exterior derivative appropriate for that form type. Specifically, if ω is a 1-form (a standard vector field), this expression states that

$$\int_{\Sigma} \nabla \times \omega \cdot \vec{n}\, dA = \oint_{\partial\Sigma} \omega \cdot d\vec{r} \qquad (2)$$

which is the classical Kelvin-Stokes theorem. Another important characteristic of differential forms is that for any k-form, ω, its exterior derivative, $d\omega$, is a (k+1)-form.

* This work performed under the auspices of the U.S. Department of Energy by Lawrence Livermore National Laboratory under Contract DE-AC52-07NA27344, UCRL LLNL-CONF-420323.

† stowell1@llnl.gov, white37@llnl.gov

Form Type	Field Type	Space	Meaning of DoF
0	Scalar	H(Grad)	Value at Point
1	Vector	H(Curl)	Path Integral Along Edge
2	Pseudo Vector	H(Div)	Surface Integral Over Face
3	Scalar Density	L_2	Volume Integral Over Cell

Table 1: This table lists the type of field that each form type is best suited for, the Hilbert space that the basis functions belong to, and how the degrees of freedom are computed.

Discrete Differential Forms [1][2], see Table 1, are finite element basis functions designed to satisfy the same differential and integral relations as their continuous counterparts. To achieve this the degrees of freedom of a k-form are associated with topological entities of dimension k: 0-forms are associated with nodes, 1-forms with edges, etc.. The value assigned to a degree of freedom (DoF) is the integral of the field over the corresponding entity: 0-form DoFs are point-wise evaluations of the field at the nodes, 1-form DoFs are line integrals along edges, etc.. These degree of freedom assignments make certain integrals trivial to compute. For example the surface integral of a 2-form field can simply be computed by summing up the DoF values from a series of faces approximating the surface of interest.

Form Type	Field Type	Exterior Derivative	Weak Derivative
0	Scalar	$\nabla \mapsto T_{01}$	None
1	Vector	$\nabla\times \mapsto T_{12}$	$\nabla\cdot \mapsto M_0^{-1}T_{01}^T M_1$
2	Pseudo Vector	$\nabla\cdot \mapsto T_{23}$	$\nabla\times \mapsto M_1^{-1}T_{12}^T M_2$
3	Scalar Density	None	$\nabla \mapsto M_2^{-1}T_{23}^T M_3$

Table 2: This table lists the discrete derivative operators appropriate for each form type. Where M_p is a p-form mass matrix and T_{pq} is a topological derivative matrix acting on p-forms and producing q-forms.

Certain derivative operators, see Table 2, are also quite simple to apply. This stems from the generalized Stokes' theorem, equation (1). Consider the Curl of a 1-form, equation (2) shows that the 2-form DoF of $\nabla\times\omega$ on a particular face is simply a linear combination of the 1-form DoFs of ω which form the boundary of that face. For first order basis functions the coefficients are just ± 1. These coefficients are chosen to produce the correct orientation of the path for the line integral. In fact the Gradient of a 0-form, the Curl of a 1-form, and the Divergence of a 2-form can all be computed in this manner. These derivatives only require knowledge of the topology of the mesh and not its geometry. This follows from the fact that the geometry is incorporated into the value of the degree of freedom itself.

An important consequence of this separation of the geometry and topology of the mesh is that certain vector calculus identities can be satisfied to machine precision. Specifically, the identities $\nabla\times\nabla\phi = 0$ for all scalar functions ϕ and $\nabla\cdot\nabla\times\vec{F} = 0$ for all vector functions $\vec{F}$ are precisely reproduced by the discrete operators T_{pq}, i.e. the matrix products $T_{12}T_{01}$ and $T_{23}T_{12}$ are equal to zero to machine precision.

For a more complete treatment of discrete differential forms see [3].

Example Problem

Consider a laser target chamber, which is roughly cylindrical with a height of nearly one meter and a radius of one meter. The chamber also has several port holes for diagnostic equipment as well as the input port for the laser beam. When a high power laser beam enters the chamber and strikes its target, it will partially vaporize the target and generate a flux of electrons which are propelled towards the outer walls of the chamber.

The charge packet in the simulations that will be discussed consists of 10^{12} electrons moving at essentially the speed of light from a target post in the center of the chamber towards the wall on the right in the upcoming images. The maximum current was 1.5 kA. The packet fans out in a conical shape as it progresses and has a Gaussian shape along the direction of propagation with a full width at half maximum of 3 cm. Therefore we expect the signal to have significant frequency content out to roughly 4.5 GHz.

We are primarily interested in the pulse of electromagnetic waves radiated by this charge packet so we do not model the incoming laser beam or the vaporization of the target. Also, we do not currently attempt to model the charge packet as a plasma, it is simply a known charge density moving through the mesh in a prescribed fashion. This approximation is valid for this particular problem because the liberated electrons have very high energies.

SOLUTION TECHNIQUES

Typical E/B Formulation

As mentioned previously a standard E/B formulation [4][5][6] of the problem requires that $\vec{J}$ be approximated by discrete 1-forms with degrees of freedom on the edges of the mesh.

$$\frac{\partial}{\partial t}\left(\epsilon\vec{E}\right) = \nabla\times\frac{1}{\mu}\vec{B} - \vec{J}$$
$$\frac{\partial}{\partial t}\vec{B} = -\nabla\times\vec{E}$$

In discrete form these equations become:

$$\begin{aligned} M_1(\epsilon)\frac{e_{n+1}-e_n}{\Delta t} &= T_{12}^T M_2(\mu^{-1}) b_{n+\frac{1}{2}} - M_1 j_{n+\frac{1}{2}} \\ \frac{b_{n+\frac{3}{2}}-b_{n+\frac{1}{2}}}{\Delta t} &= -T_{12} e_{n+1} \end{aligned}$$

Where $M_p(\alpha)$ represents a mass matrix computed using p-form basis functions and a material parameter α, T_{12} is the discrete Curl operator shown in Table 1, and lower case letters with subscript n, for example, obviously represent vectors of degrees of freedom at time $n\Delta t$.

If we take the divergence of Ampère's law and make use of the fact that the charge density is related to the electric displacement via $\nabla \cdot \vec{D} = \rho$, we derive the charge conservation equation:

$$\frac{\partial \rho}{\partial t} + \nabla \cdot \vec{J} = 0.$$

In discrete form this becomes:

$$\frac{1}{\Delta t} M_0 \left(\rho_{n+1} - \rho_n\right) + T_{01}^T M_1 j_{n+\frac{1}{2}} = 0$$

Where ρ_n is a 0-form, i.e. nodal, representation of the charge density at time $n\Delta t$. The divergence of a 1-form can only be defined in a weak sense, i.e. as a type of least squares best fit. Hence this continuity equation for the electric charge may not be locally satisfied everywhere although it should be nearly satisfied globally.

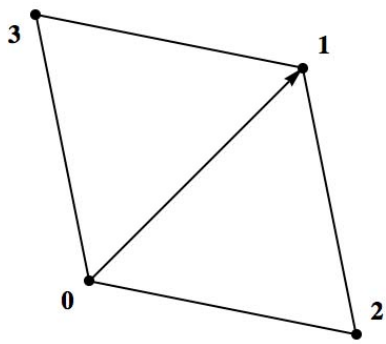

Figure 1: A toy problem illustrating the difficult of moving a charge density from one node to another using only a current density on the edge shared by the two nodes.

Consider the seemingly simple problem of moving a charge from one node to another along a particular edge of a mesh as shown in Figure 1. How much current density should be applied to the edge connecting nodes 0 and 1 to move all of the charge density from node 0 to node 1? Even this simple, two element, problem is over determined and cannot be solved.

$$\begin{aligned} \rho_n &= (\tilde{\rho}_0, 0, 0, 0) \\ \rho_{n+1} &= (0, \tilde{\rho}_1, 0, 0) \\ j_{n+\frac{1}{2}} &= (\tilde{j}_{01}, 0, 0, 0, 0) \end{aligned}$$

We have two unknowns; the charge density $\tilde{\rho}_1$ deposited on node 1, and the current density $\tilde{j}_{n+\frac{1}{2}}$, but we have four equations leading to insolubility. This toy problem, even if it could be solved, would be difficult to efficiently extend to realistic situations involving charge densities traversing meshes in three space dimensions.

The simplest method to implement this type of current source is to simply compute the current density on each edge as the projection of a prescribed function onto the edges of the mesh and hope that the continuity equation will be satisfied closely enough that the errors will not be noticeable. In many cases this does indeed work well enough.

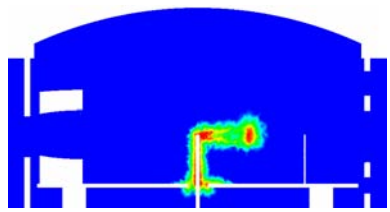

(a) Standard E/B Formulation

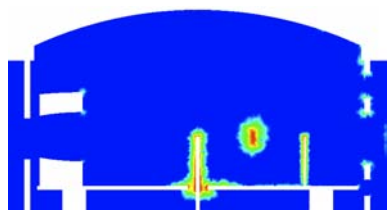

(b) E/B with Divergence Cleaning

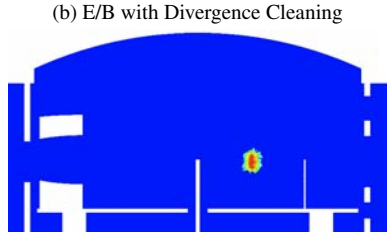

(c) D/H Formulation with PIC Source

Figure 2: The Divergence of the vector field $\vec{D}$ plotted on a logarithmic scale.

Figure 2a shows an example of a charge density plot for our model problem. The image clearly shows the charge packet itself just to the right of center. Unfortunately, it also shows a large non-physical charge buildup left behind in the wake of the packet. The boundary of the computational domain is assumed to be a perfect electrical conductor so the charge near the boundary can be interpreted as being related to the surface charge density. This is actually another oddity of the E/B formulation, surface charges appear smeared into the volume elements which touch the surface. This may not be an attractive feature of the image but at least it has a reasonable physical interpretation.

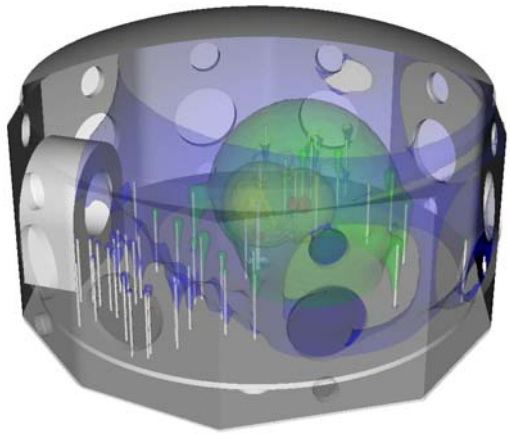

Figure 3: Logarithmically scaled contour plot of the magnitude of the electric field computed using the E/B formulation with divergence cleaning.

Divergence Cleaning

The non-physical charge buildup can be removed by performing divergence cleaning when deemed necessary or perhaps even at every time step. This is the process of adding something to the field so that its divergence has a desired value but its curl remains unchanged [7][8][9]. For the model problem we can add a $\vec{\tilde{J}}$ to the source so that the divergence will match the desired change in charge density given by $\dot{\bar{\rho}}$. We assume that the correction to $\vec{J}$ is the gradient of a scalar field ψ so that it will have zero curl.

$$\begin{aligned}
\dot{\rho} &= -\nabla\cdot\vec{J} \text{ (the } \textit{computed} \text{ change in } \rho) \\
\dot{\bar{\rho}} &= \dot{\rho}+\dot{\tilde{\rho}} = -\nabla\cdot\vec{J}-\nabla\cdot\vec{\tilde{J}} \text{ (the } \textit{desired} \text{ change)} \\
\nabla\cdot\vec{\tilde{J}} &= -\dot{\tilde{\rho}}-\nabla\cdot\vec{J} \text{ (the necessary correction to } \vec{J}) \\
\nabla^2\psi &= -\dot{\tilde{\rho}}-\nabla\cdot\vec{J}
\end{aligned}$$

In discrete form this becomes:

$$\begin{aligned}
S_0\psi &= -M_0\dot{\bar{\rho}}-T_{01}^T M_1 j_{n+\frac{1}{2}} \\
\tilde{j}_{n+\frac{1}{2}} &= T_{01}\psi
\end{aligned}$$

Where S_0 is the 0-form stiffness matrix. Each divergence cleaning operation then requires an additional linear solve to compute the scalar field ψ. It should be noted that it is generally more difficult to solve a stiffness matrix than a mass matrix so obtaining this correction is not a trivial computation in comparison to updating the electric field at each time step using Ampère's law.

With this correction we see that the divergence of $\vec{D}$, shown in figure 2b, now matches the desired charge density. Again, note that the charge density near the surfaces is due to the presence of a surface charge density.

Unfortunately, this method has a drawback when the charge density has a velocity near the speed of light. The correction introduces a small quasi-static field centered on the charge density, which appears to propagate faster than the speed of light. Figure 3 shows a logarithmically scaled contour plot of the electric field magnitude which clearly shows contours well beyond the charge packet, which is located near the innermost contour. In figure 2b this component of the field can also be seen because it introduces surface charge densities on the metal object ahead of the charge packet and on several sharp corners farther away. These non-physical charge densities are obviously due to the global solve necessary to compute ψ.

D/H Formulation

Obviously, the difficulties discussed in this paper stem from the treatment of $\vec{J}$ as a 1-form vector field. Current density is, however, a flux vector, i.e. the amount of charge crossing a given area per unit time. Flux vector fields are more naturally described using 2-forms, so we should have more luck if we approximate Ampère's law using discrete 2-forms.

$$\begin{aligned}
\frac{\partial}{\partial t}\left(\mu\vec{H}\right) &= -\nabla\times\frac{1}{\epsilon}\vec{D} \\
\frac{\partial}{\partial t}\vec{D} &= \nabla\times\vec{H}-\vec{J}
\end{aligned}$$

In discrete form these become:

$$\begin{aligned}
M_1(\mu)\frac{h_{n+1}-h_n}{\Delta t} &= -T_{12}^T M_2(\epsilon^{-1})d_{n+\frac{1}{2}} \\
\frac{d_{n+\frac{3}{2}}-d_{n+\frac{1}{2}}}{\Delta t} &= T_{12}h_{n+1}-j_{n+1}
\end{aligned}$$

In this formulation the curl of $\vec{D}$ must be computed in the weak sense. This weak form requires the solution of a linear system to update $\vec{H}$ using Faraday's law. In the standard E/B formulation it is the curl of $\vec{B}$ that must be computed in the weak sense, requiring a linear solve in Ampère's law to update $\vec{E}$. Normally this linear solve allows us to apply voltage boundary conditions on $\vec{E}$ where we can specify that the tangential component of $\vec{E}$ is zero on perfect electrical conductors. In the D/H formulation this constraint becomes unnecessary because the natural boundary condition is that the tangential component of $\nabla\times\vec{H}=0$ but, of course, this equation is consistent with the tangential component of $\vec{E}=0$ on the boundary (assuming that, on the boundary, $\hat{n}\times\vec{E}=0$ at time $t=0$ and $\hat{n}\times\vec{J}=0$ for all time.)

Simply treating $\vec{J}$ as a 2-form does not magically solve all of our problems. What it does is convert our charge buildup problem from a global least-squares fit into much more simple local charge conservation problem. Computing the divergence of Ampère's law in discrete form now leads to:

$$\frac{1}{\Delta t}\left(\rho_{n+\frac{3}{2}}-\rho_{n+\frac{1}{2}}\right)+T_{23}j_{n+1}=0.$$

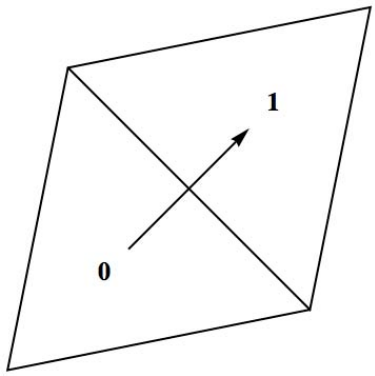

Figure 4: A toy problem illustrating the problem of moving a charge density from one element to another using only a current density on the face shared by the two elements.

Now our toy problem can be expressed in terms of a charge moving from one element to another, see Figure 4, by crossing the face shared by the elements. The problem is now well defined.

$$\begin{aligned} \rho_{n+\frac{1}{2}} &= (q_0, 0) \\ \rho_{n+\frac{3}{2}} &= (0, q_1) \\ j_{n+1} &= (I_{01}, 0, 0, 0, 0) \\ T_{23} &= \begin{pmatrix} 1 & 1 & 1 & 0 & 0 \\ -1 & 0 & 0 & 1 & 1 \end{pmatrix} \end{aligned}$$

We still have two unknowns; the amount of charge deposited in element 1, and the current crossing the intervening face. However, we now have only two equations

$$\begin{pmatrix} 0 \\ q_1 \end{pmatrix} + \Delta t \begin{pmatrix} I_{01} \\ -I_{01} \end{pmatrix} = \begin{pmatrix} q_0 \\ 0 \end{pmatrix}$$

which in this case stipulate that the current is given by $I_{01} = q_0/\Delta t$ and the charge in element 1 is $q_1 = \Delta t I_{01}$ or simply $q_1 = q_0$. This trivial solution is exactly what we would expect and it is as simple as our intuition would suggest.

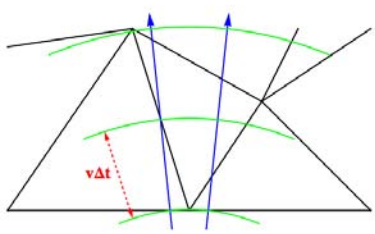

Figure 5: An example mesh illustrating charge carrying rays piercing the faces of an irregular mesh. The curved contours represent the locations at which the current fluxes must be computed as the charges progress through the mesh.

To extend this solution method to a realistic three dimensional mesh is fairly straightforward. One way to accomplish this is to use a particle-in-cell (PIC) technique. For our purposes a very rudimentary PIC method will suffice. Simply split up the trajectory of the charge packet into a group of rays and imagine the charges themselves as beads moving along these rays. At each time step we compute the fraction of each charge which crosses each face to compute the total current density. The use of fractional charges serves two purposes; to smooth out the charge packet even in coarse meshes, and more importantly to account for irregular mesh spacings. Figure 5 demonstrates a typical situation.

To achieve charge conservation we must ensure that the total amount of charge entering an element equals the that leaving. The use of rays makes this much easier as we can then require that the rays will enter and exit each element through unique faces rather than allowing charges to split and leave through two different faces. Of course this is a simplification which would have to be removed in a proper PIC simulation. The problem of charge conservation then becomes one of choosing current fluxes $I_i(t)$ which satisfy:

$$\sum_{n=0}^{N} I_i(n\Delta t) = \sum_{n=0}^{N} I_j(n\Delta t)$$

Where indices i and j indicate any two faces pierced by a particular ray and $T = N\Delta t$ is chosen large enough that the charge packet will have passed both faces by time T (we must also assume that $I_i(0) = 0$ for all faces but this is certainly reasonable.) If we use the first face pierced by the ray as a reference and label it with index 0 we can then chose all other current fluxes along that ray to be:

$$I_i(t) = \alpha_i I_0(t - n_i\Delta t) + (1 - \alpha_i) I_0(t - (n_i + 1)\Delta t)$$

Where n_i is the integer part of $d_i/(v\Delta t)$, α_i is the fractional part, d_i is the distance from face 0 to face i, and v is the speed of the charge packet. With these choices it is easy to show that the total current crossing each face along a particular ray, given by the above sums, must be equal aside from numerical errors due to finite precision arithmetic.

If enough rays are used and there are enough beads strung along each ray, then the source will appear reasonably smooth. The simulation discussed in this paper required fewer than 250 rays with 160 charges along each (i.e. less than 40,000 particles) to achieve acceptable results. We should emphasize that this does not constitute a self-consistent PIC simulation. The fields do not effect the motion of the charge packet in any way. We are simply using the PIC concept as a bookkeeping scheme to maintain charge conservation. Although this rigid beam approximation is valid for our test problem it is not a requirement of this method. The accuracy, and ease of implementation, of this method relates to the identification of the degrees of freedom of $\vec{J}$ with the precise values of the charge fluxes across the mesh faces. In a more elaborate PIC simulation these fluxes could still be used to precisely balance the

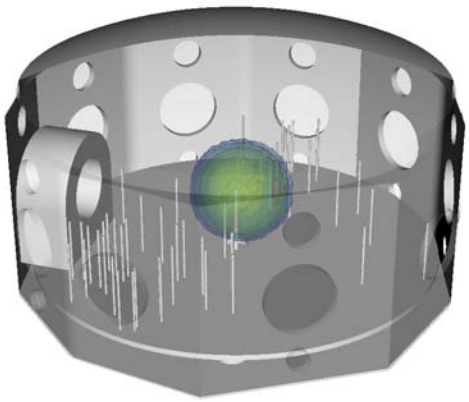

Figure 6: Logarithmically scaled contour plot of the magnitude of the electric field computed using the D/H formulation with a PIC source.

charges within each element although the bookkeeping and charge balance equations would become more complicated.

Figure 2c shows a charge density plot produced using this scheme. Clearly the image shows no sign of non-physical charge buildup. Additionally, the surface charge density does not appear. A further advantage of this method is that the charge density and current density on the surface of perfect electrical conductors can be more accurately computed, if desired. These surface fields can be directly computed from the surface degrees of freedom for $\vec{D}$ and $\vec{H}$ respectively.

Figure 6 again shows a logarithmically scaled contour plot of the electric field magnitude, analogous to that shown in figure 3. However, in the new plot the non-physical, quasi-static field contours are no longer present. The fields now properly propagate within a spherical shell which expands at the speed of light.

CONCLUSION

We have presented an outline for a charge conserving method of applying transient volumetric current sources to the Maxwell Equations in the time-domain. Some of the advantages of using a D/H formulation of the coupled first order wave equation have been discussed. The ability to run charge conserving simulations of transient current densities, while optionally computing accurate representations of surface currents and charge densities, is very appealing. The added benefit of more easily coupling to a PIC simulation, capable of more accurately modeling the motion of the charge packet itself, provides numerous avenues for enhancing the modeling of similar problems.

It should also be noted that the standard E/B formulation and the PIC method placed essentially equivalent demands on computing resources. Each simulation was performed using the same number processors and ran for virtually the same length of time. Conversely, the divergence cleaning procedure, using an algebraic multi-grid solver, increased the run time by a factor of roughly 2.8.

REFERENCES

[1] P. Castillo, R. Rieben, and D. White. FEMSTER: An object oriented class library of discrete differential forms. In *Proceedings of the 2003 IEEE International Antennas and Propagation Symposium*, volume 2, pages 181–184, Columbus, Ohio, June 2003.

[2] P. Castillo, J. Koning, R. Rieben, and D. White. A discrete differential forms framework for computational electromagnetics. *Computer Modeling in Engineering & Sciences*, 5(4):331–346, 2004.

[3] Douglas N. Arnold, Richard S. Falk, and Ragnar Winther. Finite element exterior calculus, homological techniques, and applications. *Acta Numerica*, 15:157–256, 2006.

[4] D. White and M. Stowell. Full-wave simulation of electromagnetic coupling effects in RF and mixed signal IC's. *IEEE Trans. Microwave Theory Tech.*, 52(5):1404–1413, 2004.

[5] R. Rieben, D. White, and G. Rodrigue. A high order mixed vector finite element method for solving the time dependent Maxwell equations on unstructured grids. *J. Comput. Phys.*, 204:490–519, 2005.

[6] D. White, J. Koning, and R. Rieben. Development and application of compatible discretizations of Maxwell's equations. In D. Arnold, P. Bochev, R. Lehoucq, R. Nicolaides, and M. Shaskov, editors, *Compatible Spatial Discretizations*, volume 142 of *The IMA Volumes in Mathematics and its Applications*, pages 209–238. Springer, Berlin, 2006.

[7] G.B. Jacobs and J.S. Hesthaven. Implicit-explicit time integration of a high-order particle-in-cell method with hyperbolic divergence cleaning. *Computer Physics Communications*, 180(10):1760 – 1767, 2009.

[8] C.-D. Munz, P. Omnes, R. Schneider, E. Sonnendrücker, and U. Voß. Divergence correction techniques for maxwell solvers based on a hyperbolic model. *J. Comput. Phys.*, 161(2):484–511, 2000.

[9] C. D. Munz, P. Ommes, and R. Schneider. A three-dimensional finite-volume solver for the maxwell equations with divergence cleaning on unstructured meshes. *Computer Physics Communications*, 130(1-2):83 – 117, 2000.